J. Fluid Mech. (1981), *vol.* 107, *pp.* 281–296
Printed in Great Britain

The interaction between stirring and osmosis. Part 2

By T. J. PEDLEY

Department of Applied Mathematics and Theoretical Physics, University of Cambridge

(Received 3 July 1980)

A semipermeable membrane forms part of a plane boundary which separates pure solvent from a solution of concentration C_b. Stirring motions in the solution cause it to flow parallel to the plane with uniform wall shear rate α. The velocity of osmotic solvent flow across the membrane into the solution at any point is $P\Delta C$, where P is the osmotic permeability of the membrane and ΔC is the local concentration difference across it. ΔC is reduced below C_b by a position-dependent factor γ because of the concentration boundary layer over the membrane, which is thicker than in the absence of osmosis as a result of advection by the osmotic flow itself. The concentration boundary layer is analysed, on the assumption that it is two-dimensional, for both small and large values of the dimensionless longitudinal co-ordinate

$$\xi = PC_b(9x/\alpha D^2)^{\frac{1}{3}},$$

where x is the dimensional co-ordinate and D is the solute diffusivity. These expansions are used to compute γ_l, the average value of the flux-reduction factor γ over the whole membrane, as a function of β', which is the value of ξ at the downstream end of the layer, $x = l$. It is shown that the standard physiological model, in which the layer has a given thickness δ and the stirring motions are not explicitly considered, gives accurate results for γ_l as a function of $\beta = PC_b\delta/D$ as long as δ is given by

$$\delta = 1{\cdot}22\,(Dl/\alpha)^{\frac{1}{3}},$$

so that β is proportional to β'.

1. Introduction

When pure solvent is separated from a solution with non-zero solute concentration C_b by a semipermeable membrane, there is an osmotic flow of solvent across the membrane towards the solution. The solvent flux per unit area, J, is given by

$$J = P\Delta C, \tag{1.1}$$

where ΔC is the concentration difference between fluid elements on either side of the membrane and in contact with it, and P (a constant) is the osmotic permeability of the membrane. This flux is reduced below PC_b because the osmotic flux itself advects solute away from the membrane, forming a concentration boundary layer of solute-depleted fluid; the extent of the reduction depends upon the interaction between the osmotic flow and any stirring motions that are present in the bulk solution, tending to inhibit the outward flow of solute. In a recent paper (Pedley 1980; hereafter referred to as I) the concentration boundary layer and the flux reduction were investigated for the case in which the stirring motions could be modelled as two-dimensional

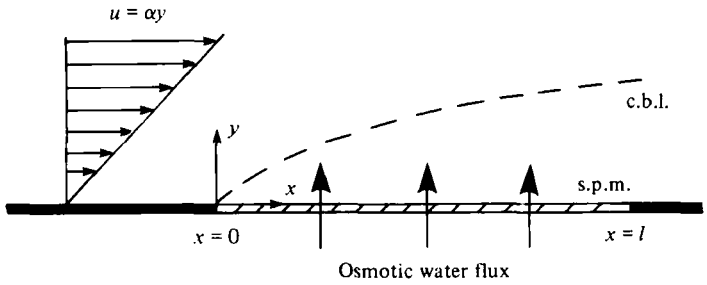

FIGURE 1. Schematic view of the problem: the semipermeable membrane (s.p.m.) forms part of the plane wall $y = 0$ and the parallel flow over it can be represented as a uniform shear, disturbed only by the osmotic flow. The thickness of the concentration boundary layer (c.b.l.) grows with x.

stagnation-point flow. In that example, the outward advection by the osmotic flow is countered by a combination of (*a*) inward advection by the normal component of the stirring velocity, and (*b*) advection along the membrane by the tangential component. In the present paper we examine a case in which the stirring motion is directed entirely parallel to the membrane, so there is no normal velocity to oppose the osmotic flux, and the concentration boundary layer is limited only by the fact that solute-poor fluid is swept along parallel to the membrane. It follows that the layer thickness will increase with downstream distance, whereas in I it was constant.

The membrane, then, is taken to form part of a solid wall ($y = 0$) past which the flow in the absence of osmosis is unidirectional, in the x direction say (figure 1). For definiteness this wall can be thought of as the wall of a two-dimensional channel or an axisymmetric tube of width $2h$, through which solution is passed at a given flow rate. The membrane will be taken to have finite length l. We shall consider only the ultimate steady-state concentration distribution, ignoring all transients. We assume that the only property of the oncoming flow that influences the concentration distribution is the shear rate at the wall, α, a constant. We further assume that boundary-layer theory is applicable. These two assumptions require that a scale for the boundary-layer thickness, δ_c, is much smaller than both l and h. Now in the absence of osmosis, a balance between advection and diffusion at a particular value of $x(< l)$ shows that

$$\delta_c \propto (Dx/\alpha)^{\frac{1}{3}}, \tag{1.2}$$

where D is the diffusivity of solute in the solvent, assumed constant. Thus $\delta_c \ll l$ for all $x < l$ as long as $\alpha l^2/D \gg 1$, and $\delta_c \ll h$ for all $x < l$ as long as $\alpha h^2/D \gg l/h$. But $\alpha h^2/D$ is the Péclet number of the oncoming flow, which is invariably large in practice because D is so small (for a typical solution, sucrose in water, $D \approx 5 \times 10^{-6}\,\mathrm{cm^2\,s^{-1}}$); thus the assumptions will hold as long as l/h is neither extremely large nor extremely small.

Implicit in the above are the two further assumptions that neither α nor δ_c is significantly affected by the presence of osmosis. In both cases this means that the osmotic flux must not be too large. One can crudely estimate that the oncoming flow will remain essentially undisturbed if the net flux of solvent through the membrane is much less than the flow rate of bulk solution down the channel or pipe; this requires that $PC_b l \ll \alpha h^2$, or

$$\beta' = PC_b \left(\frac{9l}{\alpha D^2}\right)^{\frac{1}{3}} \ll \left(\frac{h}{l}\frac{\alpha h^2}{D}\right)^{\frac{1}{3}}, \tag{1.3}$$

where the factor 9 has been introduced into β' for subsequent convenience.

A more subtle constraint is obtained by realizing that the longitudinal pressure gradient perturbation induced by a normal velocity V_0 is of order $\rho U V_0 h/l^2$, where ρ is the fluid density and U is a scale for the longitudinal velocity outside a viscous boundary layer; $U = \alpha\delta_v$, where δ_v is the viscous boundary-layer thickness. Within the boundary layer this causes a longitudinal velocity perturbation comparable with $\alpha\delta_v$ if

$$\rho\alpha\delta_v V_0 h/l^2 \sim \rho\alpha^2\delta_v^2/l.$$

Now δ_v is determined by a balance between viscous and inertia terms, so that $\delta_v \sim (\nu l/\alpha)^{\frac{1}{3}}$, where ν is the kinematic viscosity of the fluid. Thus, for the longitudinal velocity perturbation to be negligible, we require

$$V_0 \ll \frac{\alpha l}{h}\left(\frac{\nu l}{\alpha}\right)^{\frac{1}{3}}$$

(cf. Smith 1976). Alternatively, since $V_0 \sim PC_b$ here, we may write

$$\beta' \ll \left(\frac{\alpha h^2}{D}\frac{\nu}{D}\right)^{\frac{1}{3}}\left(\frac{l}{h}\right)^{\frac{1}{3}}, \tag{1.4}$$

where β' is defined in (1.3). We assume that both (1.3) and (1.4) are satisfied. Finally, whether δ_c, given by (1.2), remains a good estimate of concentration boundary-layer thickness for all $x < l$ in the presence of osmosis cannot be decided until the structure of the layer has been elucidated. Further discussion is postponed to §4.

The problem to be solved can now be formulated precisely, as follows. We seek the steady-state distribution of solute concentration $C(x, y)$ in the concentration boundary layer, $0 < x < l$, $0 < y < \infty$. In the layer the velocity field is $(u, v) = [\alpha y, J(x)]$, where $J(x)$ is the osmotic water flux per unit area of membrane, expected to vary slowly with x, so the steady convection–diffusion equation for C becomes

$$\alpha y C_x + J(x)\, C_y = D C_{yy}. \tag{1.5}$$

The boundary conditions are

$$C \to C_b \quad \text{as} \quad y \to \infty, \tag{1.6a}$$

$$DC_y = J(x)\, C \quad \text{on} \quad y = 0, \tag{1.6b}$$

$$J(x) = PC(x, 0), \tag{1.6c}$$

of which the second represents the fact that the membrane is impermeable to solute, and the third is the same as (1.1) for the case where there is no solute on the other side of the membrane. The object, as in I, is to calculate the ratio between the actual osmotic flux to that which would arise if (1.1) were applicable with $\Delta C = C_b$. Here that ratio would depend on x; we therefore seek

$$\gamma(x) = C(x, 0)/C_b. \tag{1.7}$$

A problem rather similar to the one posed here has previously been investigated in the context of 'reverse osmosis', a desalination technique. Both Gill, Tien & Zeh (1966) and Hendricks & Williams (1971) considered a concentration distribution

governed essentially by (1.5) with boundary conditions (1.6*a*) and (1.6*b*). However, $J(x)$ was not given in terms of $C(x, 0)$ by (1.6*c*), but rather by an equation of the form

$$J(x) = -P[BC_b - C(x, 0)],$$

where B is a dimensionless constant, which is large enough for J to be negative. The term involving B represents the fact that the hydrostatic pressure in the channel is greater than that outside, so that solvent is forced out across the membrane leaving the solute behind. Unfortunately this outflow causes the solute to pile up against the membrane ('concentration polarization'), and its osmotic effect inhibits the outflow. Gill *et al.* (1966) analysed this effect by means of a co-ordinate expansion for small x (cf. §2 below), while Hendricks & Williams (1971) solved the problem approximately for all x, using an integral method in which the concentration was assumed to fall off exponentially as y increased. Such a distribution agreed well with the co-ordinate expansion for small x, could be shown to agree with the exact solution for sufficiently large x, and led to excellent agreement with experiment for intermediate values. However, this success was a consequence of the fact that, with $v < 0$, solute is always advected *towards* the wall and is therefore confined to a thinner concentration boundary layer than in the absence of the transverse velocity. It has already been remarked that in the present case the solute is advected away from the wall, the concentration boundary-layer thickness must increase with x, and a simple exponential y dependence would be inadequate (as we shall see).

In the case where there is no osmotic flux, and the boundary condition at the membrane is different from (1.6*b*, *c*) (e.g. $C(x, 0) = C_1 \neq C_b$) then the problem (1.5)–(1.6) admits a similarity solution in which the appropriate normal co-ordinate is y/δ_c (Lévêque 1928). It proves to be convenient to recast the present problem in terms of Lévêque's similarity variables, and we accordingly set

$$\theta = C/C_b, \quad \eta = y(\alpha/9Dx)^{\frac{1}{3}}, \quad \xi = \beta'(x/l)^{\frac{1}{3}}, \tag{1.8}$$

where β' is given by (1.3). The equations and boundary conditions become

$$\theta_{\eta\eta} + 3\eta^2\theta_\eta - 3\eta\xi\theta_\xi = \xi\gamma(\xi)\,\theta_\eta \tag{1.9}$$

and

$$\theta(\xi, \infty) = 1, \quad \theta(\xi, 0) = \gamma(\xi), \quad \theta_\eta(\xi, 0) = \xi\gamma^2(\xi). \tag{1.10}$$

It can be seen that the parameter β' has been scaled out of the problem by incorporating it into the dimensionless co-ordinate ξ; it will of course enter into the final results because the total osmotic flux is $PC_b lw\gamma_l$, where w is the width of the membrane and

$$\gamma_l = \frac{1}{l}\int_0^l \theta(x, 0)\,dx = \frac{3}{\beta'^3}\int_0^{\beta'} \gamma(\xi)\,\xi^2\,d\xi. \tag{1.11}$$

It is worth noting that ξ is proportional to $PC_b\delta_c/D$, with δ_c given by (1.2). Hence, although it is a variable, it can be thought of as analogous to the constant parameter β' defined in I, and represents the ratio between the time taken for osmotic advection across the concentration boundary layer, and the time scale for diffusion across it.

An exact solution to the problem (1.9)–(1.10) is not available. We accordingly examine the solution separately in the two limits $\xi \to 0$ (§2) and $\xi \to \infty$ (§3), showing how they can be combined into a reasonably accurate representation of the function $\gamma(\xi)$ for all ξ of interest.

2. Expansion for small ξ

If ξ is set equal to zero in (1.9)–(1.10), it can be seen that the solution is $\theta \equiv 1$. Moreover, the form of these equations suggests that we seek an expansion in powers of ξ, of the following form

$$\theta(\xi, \eta) = 1 + \sum_{n=1}^{\infty} \xi^n \theta_n(\eta),$$
$$\gamma(\xi) = 1 + \sum_{n=1}^{\infty} \xi^n \gamma_n \tag{2.1}$$

(so that $\theta_n(0) = \gamma_n$). Substitution into (1.9)–(1.10) leads to a sequence of linear ordinary differential equations for the functions $\theta_n(\eta)$, with two-point boundary conditions. In fact we obtain

$$\theta_n'' + 3\eta^2\theta_n' - 3n\eta\theta_n = \sum_{j=1}^{n-1} \gamma_{n-j-1}\theta_j', \tag{2.2}$$

where $\gamma_0 = 1$, and the boundary conditions are

$$\left.\begin{aligned} &\theta_n(\infty) = 0 \quad (\text{all } n), \\ &\theta_1'(0) = 1, \\ &\theta_n'(0) = 2\gamma_{n-1} + 2\sum_{j=1}^{j_n} \gamma_{n-j-1}\gamma_j + k_n \quad (n > 1), \end{aligned}\right\} \tag{2.3}$$

where, if n is even, $k_n = 0, j_n = \frac{1}{2}(n-2)$, while, if n is odd, $k_n = \frac{1}{2}\gamma_{n-1}^2, j_n = \frac{1}{2}(n-3)$.

The solutions of (2.2)–(2.3) can be expressed in terms of confluent hypergeometric functions and their integrals (for example, $\theta_1 \equiv -U(1, \frac{2}{3}, \eta^3)/3\Gamma(\frac{2}{3})$ in the notation of Abramowitz & Stegun (1964, p. 504), and $\gamma_1 = -1/\Gamma(\frac{2}{3})$) but it is simpler for $n > 1$ to solve the equations numerically. The values of γ_n for $n = 0, 1, \ldots 10$ are given in table 1. The graphs of $\gamma(\xi)$ obtained by terminating the series (2.1) after different numbers of terms are shown in figure 2. Graphs such as these correspond to the results obtained in the reverse osmosis problem by Gill *et al.* (1966).

It can be seen that this series expansion is not useful for values of ξ greater than about 0·5, and the likelihood of being able to construct a composite expansion by joining this and the large-ξ expansion of §3 is very small. Indeed, the increasing magnitude of γ_n as n increases demonstrates that the series (2.1) cannot have a very large radius of convergence. However, the information about the function $\gamma(\xi)$ contained in the coefficients γ_n can be used to transform (2.1) into a series which converges for much larger values of ξ, by means of an Euler transformation (Van Dyke 1975, pp. 208 and 245–246). The alternation of signs of the γ_n suggests that the singularity nearest to the origin in the complex ξ plane lies on the negative real axis, at $\xi = -C$, say. If the nature of the singularity is such that

$$\gamma(\xi) \sim \text{const.}\,(C + \xi)^p \quad (p \neq \text{integer})$$

as $\xi \to -C$, then the coefficients of the small-ξ expansion will satisfy the relation

$$\frac{\gamma_n}{\gamma_{n-1}} \sim -\frac{1}{C}\left(1 - \frac{1+p}{n}\right)$$

n	γ_n	C_n
0	1·0	1·0
1	−0·738487	−0·5329
2	0·722595	−0·1566
3	−0·789891	−0·0772
4	0·915469	−0·0463
5	−1·099780	−0·0309
6	1·353512	−0·0222
7	−1·694905	−0·0167
8	2·150218	−0·0130
9	−2·755602	−0·0104
10	3·560127	−0·0085

TABLE 1. Coefficients of the small-ξ and small-ξ_1 expansions for $\gamma(\xi)$.

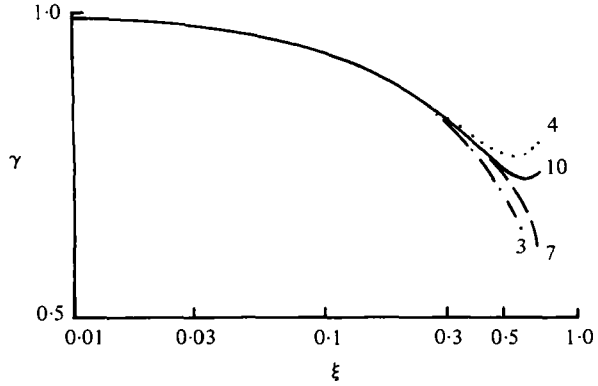

FIGURE 2. Graphs of $\gamma(\xi)$ obtained by terminating the power series (2.1) after different numbers of terms, as marked.

as $n \to \infty$. Plotting $|\gamma_n/\gamma_{n-1}|$ against $1/n$ (a 'Domb–Sykes plot': Domb & Sykes 1957) we find that the curve becomes linear as $1/n \to 0$, with an intercept on the $1/n = 0$ axis equal to $1/C$, where $C = 0{\cdot}7217$ (figure 3).

We now make the Euler transformation, and recast γ as a power series in ξ_1, where

$$\xi_1 = \frac{\xi}{C+\xi}. \tag{2.4}$$

This has the effect of banishing the singularity at $\xi = -C$ to $\xi_1 = \infty$ and, if $\gamma(\xi)$ has no other finite singularity, the only finite singularity in the ξ_1 plane will be at $\xi_1 = 1$ ($\xi = \infty$); note that we are interested only in the range $0 \leqslant \xi_1 < 1$. The power series in ξ_1 has the form

$$\gamma = 1 + \sum_{n=1}^{\infty} C_n \xi_1^n; \tag{2.5}$$

the coefficients C_n have been calculated for $n = 1, 2, \ldots, 10$ by terminating the original expansion (2.1) at $n = 10$, substituting $\xi = C\xi_1/(1-\xi_1)$ into it, and expanding the result in powers of ξ_1. The coefficients C_n so obtained are also given in table 1: these are inevitably less accurately determined than the original γ_n, so they are given to fewer significant figures. Nevertheless, they can be seen to decrease in magnitude as n

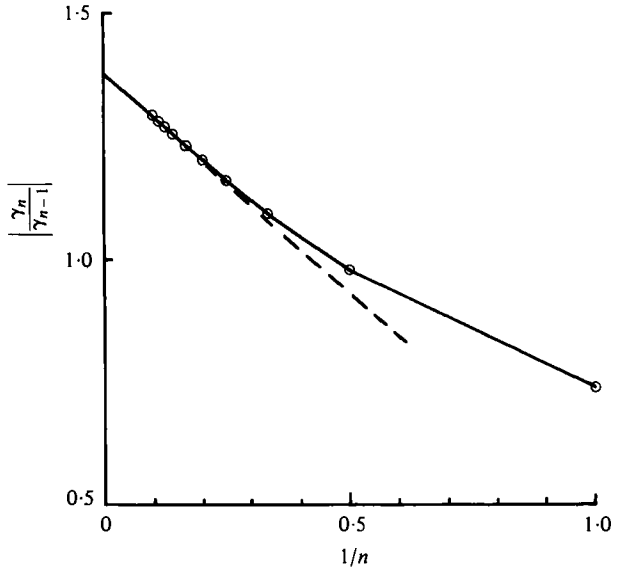

FIGURE 3. Domb–Sykes plot for the coefficients γ_n.

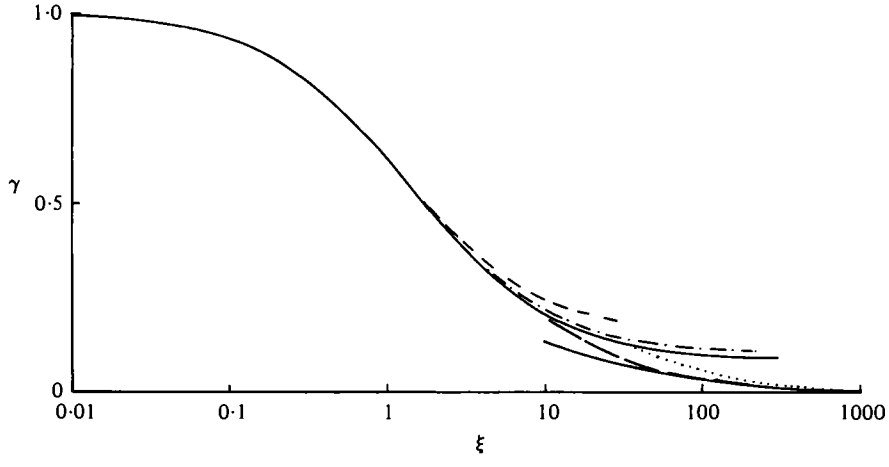

FIGURE 4. Graphs of $\gamma(\xi)$ obtained from various expansions: the two solid curves represent the series (2.5) terminated after 10 terms and the large-ξ expansion (3.17) with (3.24); ---- and -·-·-· represent (2.5) terminated after 5 terms and 8 terms respectively; ..... represents the first term of (3.17) by itself; — — — has been calculated from the implicit equation (3.23).

increases and, when a Domb–Sykes plot is drawn for the C_n, it too becomes approximately linear, with an intercept that is very close to $+1$, suggesting that the nearest singularity in the ξ_1 plane is indeed at $\xi_1 = 1$, i.e. at $\xi = \infty$. Thus the power series (2.5) is expected to be convergent for all ξ_1, and even the first ten terms will give a good asymptotic expansion for a wide range of values of ξ. This expectation is borne out by plots of γ against ξ obtained by terminating the expansion (2.5) after different numbers of terms, as shown in figure 4. The 10-term expansion differs little from the 8-term expansion, which differs little from the 5-term expansion, etc., for values of ξ

up to about 10. We assume, then, that the 10-term expansion (the solid curve) is accurate for $\xi \leqslant 10$.

3. Expansion for large ξ

In this section the function $\xi\gamma(\xi)$ is rewritten as $V(\xi)$, so the equation and boundary conditions (1.9)–(1.10) become

$$\theta_{\eta\eta} + [3\eta^2 - V(\xi)]\,\theta_\eta = 3\eta\xi\theta_\xi, \tag{3.1}$$

$$\theta(\xi,\infty) = 1, \quad \theta(\xi,0) = V(\xi)/\xi, \tag{3.2a,b}$$

$$\theta_\eta(\xi,0) = V(\xi)\,\theta(\xi,0). \tag{3.2c}$$

A model problem

Some guidance in the solution of this problem for large ξ is obtained by considering a model problem in which the right-hand side of (3.1) is omitted so that ξ is merely a parameter; θ_ξ will of course not be identically zero, but, if that term is no larger than any of the others when the model solution is substituted, then the correct solution should bear some qualitative resemblance to the model solution. Now the model problem turns out to be the same as that solved in I when the governing parameter β' was not too large: the variable η was called ζ in I, the coefficient 3 in the second term was called $\frac{1}{2}a_2$ (and took a different value), and the quantity $V(\xi)$ was called V'; we have already seen that ξ here corresponds to β' in I.

In the notation of this paper, then, the solution of the model problem can be written as an integral:

$$\theta = \frac{1}{1+AV}\left\{1 + V\int_0^\eta \exp\left(V\eta - \eta^3\right) d\eta\right\}, \tag{3.3}$$

where

$$A = \int_0^\infty \exp\left(V\eta - \eta^3\right) d\eta \tag{3.4}$$

and

$$\gamma = \frac{V}{\xi} = \frac{1}{1+AV}. \tag{3.5}$$

In this form the model solution is not very helpful, but its expansion for large V is useful. As discussed in I, the integral in (3.4) is dominated by the neighbourhood of $\eta = (\frac{1}{3}V)^{\frac{1}{2}}$ and takes the approximate value

$$A \approx \left(\frac{\pi^2}{3V}\right)^{\frac{1}{4}} \exp\left\{2(\tfrac{1}{3}V)^{\frac{3}{2}}\right\}.$$

From this, with (3.5), the leading terms of the expansion for γ as a function of ξ can be deduced:

$$V = \xi\gamma \sim 3\left(\frac{\log\xi}{2}\right)^{\frac{3}{2}}\left\{1 - \frac{\alpha_0 + \frac{7}{9}\log\log\xi}{\log\xi} + O\left[\frac{\log\log\xi}{(\log\xi)^2}\right]\right\}, \tag{3.6}$$

where $\alpha_0 = \log\left(3\pi^{\frac{1}{2}}/2^{\frac{7}{9}}\right) = 0{\cdot}941$ (cf. equation (4.17) of I). Furthermore, by expanding the integral in (3.3) appropriately, we can calculate the form that θ takes in various regions of the interval $0 \leqslant \eta < \infty$ (this was not done explicitly in I). The results are as follows, in order of increasing η.

For $\eta' = V\eta = O(1)$,

$$\theta \sim \frac{V}{\xi} e^{\eta'} [1 + O(V^{-3})]; \tag{3.7a}$$

for $\eta = O(1)$,

$$\theta \sim \frac{V}{\xi} \exp(V\eta - \eta^3)[1 + O(V^{-1})]; \tag{3.7b}$$

for $\zeta = V^{-\frac{1}{2}}\eta = O(1)$, but $\zeta < 1/\sqrt{3}$,

$$\theta \sim \frac{V}{\xi} \frac{\exp[V^{\frac{3}{2}}(\zeta - \zeta^3)]}{1 - 3\zeta^2}[1 + O(V^{-\frac{3}{2}})]; \tag{3.7c}$$

for $u = V^{\frac{1}{2}}(\zeta - 1/\sqrt{3}) = O(1)$,

$$\theta \sim \frac{V^{\frac{1}{4}}\pi^{\frac{1}{2}}}{\xi . 2(3)^{\frac{1}{4}}} \exp[2(\tfrac{1}{3}V)^{\frac{3}{2}}][1 + \operatorname{erf}(3^{\frac{1}{4}}u)][1 + O(V^{-\frac{1}{2}})]; \tag{3.7d}$$

for $\zeta = O(1)$ but $\zeta > 1/\sqrt{3}$,

$$\theta \sim 1. \tag{3.7e}$$

It is the $1/\log \xi$ terms in (3.6) that enables (3.7*d*) to tend exponentially to 1 as $u \to \infty$.

One might have anticipated on physical grounds that the concentration distribution at large V would be determined entirely advectively except in two relatively thin diffusive regions, one on the wall ($\eta' = O(1)$) and one near the location where the stream function is zero ($u = O(1)$). However, if the above solutions are substituted back into (3.1) (without its right-hand side) it can be seen that only in the outermost region, $\zeta > 1/\sqrt{3}$, is the diffusion term $(\theta_{\eta\eta} + 3\eta^2\theta_\eta)$ negligible. Thus there is no short cut to the solution in the complete problem either.

The complete problem

The model solution suggests first that an asymptotic solution to the complete problem may be found if ξ is sufficiently large that $V \gg 1$, and second that the expansion will be in terms of $\log \xi$ rather than ξ. We accordingly make the transformation $\chi = \log \xi$ so that (3.1)–(3.2) become

$$\theta_{\eta\eta} + [3\eta^2 - V(\chi)]\theta_\eta - 3\eta\theta_\chi = 0, \tag{3.8}$$

$$\theta(\chi, \infty) = 1, \quad \theta(\chi, 0) = e^{-\chi}V(\chi), \tag{3.9a,b}$$

$$\theta_\eta(\chi, 0) = V(\chi)\theta(\chi, 0); \tag{3.9c}$$

we seek V as a function of the variable χ when χ is large, on the assumption that V tends to infinity as χ does.

The concentration distributions given for the model problem by (3.7) indicate that we should attempt to solve (3.8) in a succession of regions, in each of which different terms in the equation are important. We shall work from the wall, $\eta = 0$, out to the bulk fluid, $\eta \to \infty$. First, then, we follow (3.7*a*) and, taking account of (3.9*b*), we set

$$\eta' = \eta V(\chi), \quad \theta = e^{-\chi}V(\chi)\tilde{\theta}(\chi, \eta'); \tag{3.10}$$

the equation becomes

$$\tilde{\theta}_{\eta'\eta'} - \tilde{\theta}_{\eta'} = \frac{3}{V^3}\left\{\eta'\tilde{\theta}_x - \left(1 - \frac{V'}{V}\right)(\eta'^2\tilde{\theta}_{\eta'} + \eta'\tilde{\theta})\right\}.$$

When $\eta' = O(1)$ the solution can be expanded in inverse powers of V^3, and it is a simple matter to show that the solution satisfying (3.9*b*, *c*) can be written

$$\tilde{\theta} = e^{\eta'}\left\{1+\frac{3}{V^3}\left(1-\frac{V'}{V}\right)\phi_1(\eta')+O(V^{-6})\right\}, \tag{3.11}$$

where ϕ_1 is a polynomial in η' in which the highest power is η'^3. This confirms that the expansion breaks down when $\eta' = O(V)$ or $\eta = O(1)$, as indicated already by (3.7*b*).

In the region where $\eta = O(1)$ we know that the solution must match with (3.11) as $\eta \to 0$. We therefore write

$$\theta = e^{-\chi}V(\chi)\, e^{\eta V(\chi)}\phi(\chi, \eta), \tag{3.12}$$

substitute into (3.8) and obtain

$$\phi_\eta + 3\eta^2\phi + \frac{1}{V}\left\{\phi_{\eta\eta} + 3\eta^2\phi_\eta + 3\eta\left(1-\frac{V'}{V}-\eta V'\right)\phi - 3\eta\phi_\chi\right\} = 0, \tag{3.13}$$

where ϕ must tend to 1 as $\eta \to 0$, for matching. The error in neglecting the term in curly brackets will be $O(V^{-1})$, as in (3.7*b*), as long as both V'/V and V' tend to zero as $\chi \to \infty$; this condition is satisfied if $V = O(\chi^{\frac{3}{2}})$ as suggested by (3.6). The leading term in the solution for $\eta = O(1)$ is thus given by

$$\phi = e^{-\eta^3}[1+O(V^{-1})]. \tag{3.14}$$

This solution breaks down when $\eta = O(V^{\frac{1}{2}})$, because the neglected term $(3\eta^2/V)\phi_\eta$ becomes as large as the retained term ϕ_η in this region.

The next region to examine therefore is that in which $\zeta = V^{-\frac{1}{2}}(\chi)\,\eta$ is $O(1)$ (cf. (3.7*c*)); the equation for θ, transformed accordingly, then becomes

$$V^{-\frac{3}{2}}\theta_{\zeta\zeta} + \left[3\zeta^2\left(1+\frac{V'}{2V}\right)-1\right]\theta_\zeta - 3\zeta\theta_\chi = 0.$$

Now, the solution must match with that obtained from (3.12) and (3.14) as $\zeta \to 0$, which suggests taking out a factor $\exp[V^{\frac{3}{2}}(\zeta-\zeta^3)]$, as in (3.7*c*). However, the coefficient of θ_ζ in the equation suggests a slightly different factor and, although V'/V is assumed to be small, $V^{\frac{1}{2}}V'$ may not be, so we set

$$\theta = e^{-\chi}V(\chi)\exp\left\{V^{\frac{3}{2}}(\chi)\left[\zeta-\left(1+\frac{V'}{2V}\right)\zeta^3\right]\right\}\psi(\chi, \zeta), \tag{3.15}$$

where $\psi \to 1$ as $\zeta \to 0$ for matching. The equation for ψ is then

$$\begin{aligned}(1-3\zeta^2)\psi_\zeta - 3\zeta\psi - \tfrac{9}{2}V^{\frac{1}{2}}V'(\zeta^2-\zeta^4)\psi \\ = 3\zeta\psi_\chi + \frac{V'}{2V}\{3\zeta^2\psi_\zeta + 12\zeta\psi\} - 3\frac{d}{d\chi}\left(\frac{V^{\frac{1}{2}}V'}{2}\right)\zeta^4\psi - V^{-\frac{3}{2}}\psi_{\zeta\zeta}.\end{aligned} \tag{3.16}$$

All the terms on the right-hand side of this equation are expected to be small, because V'/V is assumed small and ψ_χ is likely to be small because of the χ-independent matching condition as $\zeta \to 0$. On the left-hand side, the term involving $V^{\frac{1}{2}}V'$ cannot be large because the leading term for ψ would then have to be identically zero. Hence we expect that $V^{\frac{1}{2}}V'$ is approximately a constant, which may be zero. If the constant is not zero, this means that, as $\chi \to \infty$, $V \propto \chi^{\frac{3}{2}}$, which is consistent with (3.6). We therefore suppose that

$$V(\chi) = (k\chi)^{\frac{3}{2}}[1+g(\chi)], \tag{3.17}$$

where $g(\chi) = o(1)$ as $\chi \to \infty$. The equation for the leading term in ψ is then, from (3.16),

$$(1-3\zeta^2)\psi_\zeta - 3\zeta\psi - 3k(\zeta^2-\zeta^4)\psi = 0;$$

the solution of this that tends to 1 as $\zeta \to 0$ is

$$\psi = \frac{\exp[-\frac{1}{3}k(2\zeta-\zeta^3)]}{(1-3\zeta^2)^{\frac{1}{2}}}\left(\frac{1+\sqrt{3}\zeta}{1-\sqrt{3}\zeta}\right)^{k/3^{\frac{1}{2}}}. \tag{3.18}$$

The next term in the expansion for ψ will be $O(V'/V) = O(V^{-\frac{1}{2}})$, from (3.16), as in (3.7*c*).

This solution shows that as in the model problem a singularity occurs at $\zeta = 1/\sqrt{3}$, around which the concentration gradient becomes high. Following (3.7*d*), we set

$$u = V^{\frac{1}{2}}(\zeta - 1/\sqrt{3})$$

and the equation for θ becomes

$$\theta_{uu} + 2\sqrt{3}u\theta_u = \sqrt{3}\theta_\chi + O(V^{-\frac{1}{2}}). \tag{3.19}$$

The solution must tend exponentially to 1 as $u \to +\infty$, and must match with (3.18) as $u \to -\infty$; it is this matching which will determine the constant k and the leading terms of the function $g(\chi)$ in equation (3.17). Neglecting the right-hand side of (3.19) we find the solution which tends to 1 as $u \to +\infty$ is

$$\theta = \tfrac{1}{2}\{1 + \operatorname{erf}(3^{\frac{1}{2}}u)\}, \tag{3.20}$$

as in (3.7*d*). As $u \to -\infty$ this gives

$$\theta \sim \frac{e^{-\sqrt{3}\,u^2}}{2\pi^{\frac{1}{2}}3^{\frac{1}{2}}(-u)}. \tag{3.21}$$

The $1/(-u)$ dependence here can match with (3.18) only if $k = \frac{1}{2}3^{\frac{3}{2}}$, in which case (3.18) becomes

$$\psi = \frac{\exp[-\sqrt{3}(\zeta - \frac{1}{2}\zeta^3)]}{1-\sqrt{3}\zeta}. \tag{3.22}$$

Note that this value of k means that the leading term of $V(\chi)$ is *exactly* the same as in the model problem (equation (3.6)). Matching of (3.21) with the form of θ given by (3.15) and (3.22) now gives the following relation between V and χ:

$$V^{\frac{7}{4}}\exp[2(V/3)^{\frac{3}{2}}] = \frac{3^{\frac{1}{4}}}{2\pi^{\frac{1}{2}}}e^{\chi+1}, \tag{3.23}$$

which can be expanded to give (3.17) with

$$g(\chi) = -\frac{1}{\chi}(\alpha_1 + \tfrac{7}{6}\log\chi) + O\left(\frac{\log\chi}{\chi^2}\right), \tag{3.24}$$

where

$$\alpha_1 = \log(3\pi^{\frac{1}{3}}2^{-\frac{1}{6}}e^{-\frac{2}{3}}) = 0{\cdot}737.$$

This constant α_1 is different from the constant α_0 appearing in (3.6), but otherwise the solution of the complete problem is the same as that of the model problem, to this order in the determination of $\gamma(\chi)$.

The large-ξ expansion of $\gamma(\xi)$, obtained from (3.6) with α_1 for α_0, is plotted on figure 4, together with its leading term; also plotted is the curve obtained directly from (3.23). The latter can be seen to lie between the others and to join up fairly

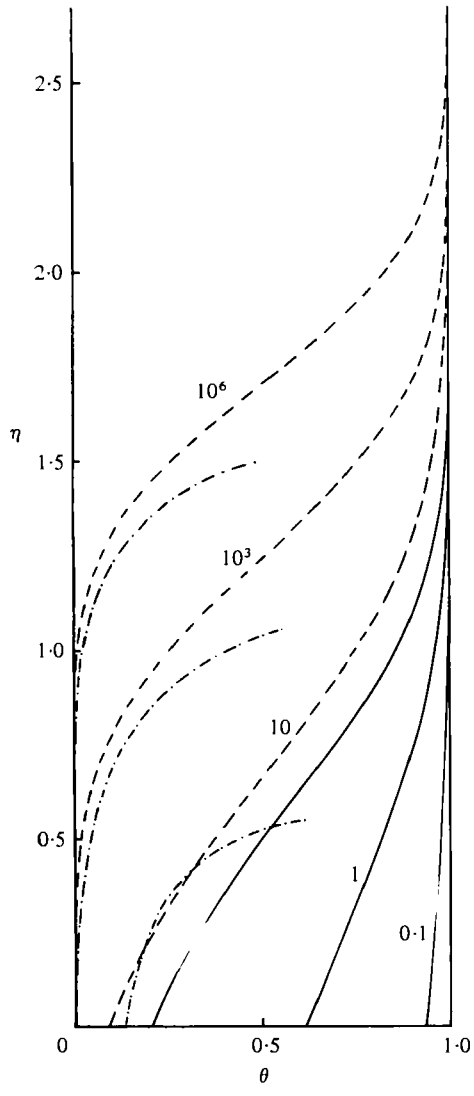

FIGURE 5. Concentration distribution $\theta(\xi, \eta)$ plotted against η for various values of ξ, as marked. ———, small-ξ expansion; – – – –, large-ξ expansion, equation (3.20); –·–·–, large-ξ expansion, equations (3.15) and (3.18).

smoothly with the small-ξ expansion, at $\xi = 10$. We therefore take (3.23) to be reasonably accurate for practical purposes when $\xi > 10$, while the 10-term expansion (2.5) is accurate for $\xi < 10$.

4. Discussion

The reasonable proximity of the large- and small-ξ expansions for γ when ξ is in the range $10 \leqslant \xi \leqslant 40$ could be merely fortuitous. As a test, therefore, the full concentration distributions $\theta(\xi, \eta)$ predicted by the two expansions have been plotted for $\xi = 10$ on figure 5, along with the distributions for other values of ξ predicted by only one expansion. It can be seen that the outermost approximation for the large-ξ

expansion (equation (3.20): broken curve) agrees rather well in shape with the small-ξ expansion, calculated as a power series in ξ_1 (cf. equation (2.5); solid curve); this small-ξ expansion is expected to be accurate for $\xi = 10$. The correction to (3.20) at small η, represented by equations (3.15) and (3.18) and plotted as the dash–dot curve, does not make much difference except in the detailed concentration adjustment near the wall. We conclude that even the large-ξ expansion gives a qualitatively correct picture of the concentration distribution for $\xi = 10$, although χ is only 2·3.

From figure 5 one can also see how the concentration distribution changes as ξ is increased. The point of inflection at $\eta = (\frac{1}{3}V)^{\frac{1}{2}}$ ($u = 0$), where the concentration gradient is steepest, becomes more marked and moves further out. For smaller values of η, outwards advection of solute-poor fluid by the osmotic flow is dominant, while for larger values of η the downstream advection by the primary flow is dominant. The regions where diffusion is most important are the neighbourhood of the inflection point ($u = O(1)$; equation (3.19)) and very near the wall ($\eta' = O(1)$; equation (3.10)), although it is not negligible in between. It can be seen that the matching between the large-η solution (3.20) and the smaller-η solutions (3.15) and (3.18), which is vital for the determination of γ, is not perfectly smooth even when ξ is as large as 10^6; the reason is that V is still only 8·7 and $V^{\frac{1}{2}}$ (assumed large) only 1·7. If V were large, moreover, we see that the concentration distribution would extend to a distance $O(\delta_c V^{\frac{1}{2}})$ from the wall ($\zeta = O(1)$), but the fact that $V^{\frac{1}{2}}$ is only about 3 when $\xi = 10^6$ means that δ_c remains an appropriate scale for the concentration boundary-layer thickness (cf. § 1).

In an experiment designed to measure the osmotic permeability P of the membrane one measures the total osmotic flux lwJ_T across the whole membrane, length l and width w, and hopes to infer P from a theoretical relationship between P, J_T and the driving concentration difference C_b. The crudest example of such a relationship would be (1.1) with $\Delta C = C_b$. Now J_T is equal to $PC_b\gamma_l$, where γ_l is given by (1.11), which in turn gives

$$J_T = \left(\frac{\alpha D^2}{9l}\right)^{\frac{1}{3}} \beta' \gamma_l \tag{4.1}$$

from (1.3). Thus one effectively measures $\beta'\gamma_l$ and wishes to infer β' from a theory which takes account of the concentration boundary layer. As explained in I, the standard physiological model of the boundary layer ignores the stirring motions and postulates a given layer thickness δ; this model yields the theoretical result

$$\gamma_l = e^{-\beta\gamma_l}, \tag{4.2}$$

where

$$\beta = PC_b\delta/D. \tag{4.3}$$

It would be very convenient if this equation could still be used to describe the effect of the layer, at least approximately, when stirring is properly taken into account. It was shown in I that (4.2) *can* be used in the case of stirring by stagnation-point flow, with excellent accuracy for realistic parameter values, if δ is given by

$$\delta = 1{\cdot}59\left(\frac{D}{\nu}\right)^{\frac{1}{3}}\left(\frac{\nu}{\bar{\alpha}}\right)^{\frac{1}{2}},$$

where ν is the kinematic viscosity of the fluid and $\bar{\alpha}$ is the stirring parameter. The

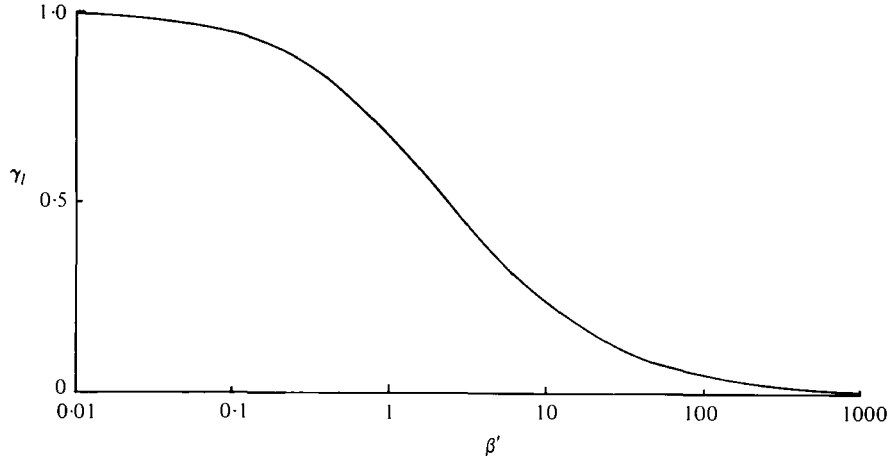

FIGURE 6. Graph of γ_l, defined by (1.11), against β', defined by (1.3).

β' or β''	γ_l, present theory	γ_l, from (4.2)
0·01	0·995	0·994
0·05	0·973	0·972
0·1	0·949	0·946
0·5	0·798	0·793
1·0	0·678	0·674
5·0	0·353	0·354
10·0	0·248	0·242
50·0	0·083	0·084
100·0	0·049	0·051
500·0	0·012	0·014

TABLE 2. Comparison of the values of γ_l predicted for various values of β' from figure 6, and those predicted for the same values of β'' ($= \beta/0{\cdot}586$) from (4.2).

dimensional terms in this expression give a scale for the concentration boundary-layer thickness in the absence of osmosis, when the Schmidt number ν/D is large.

In the present case of 'parallel-flow stirring' the scale for the concentration boundary-layer thickness (δ_c, equation (1.2)) varies with x, but a representative value for the whole membrane, $\overline{\delta_c}$, can be obtained by putting $x = l$ in this equation. It can be seen that β', given by (1.3), is analogous to β, given by (4.3), but with $9\frac{1}{3}\overline{\delta}_c$ in place of δ. Thus we must see if the relationship between γ_l and β' predicted by the present theory can be accurately represented by (4.2) with β equal to some multiple of β'. First, then, we must compute γ_l, given by (1.11), as a function of β'. This has been done numerically using the above results. For $0 < \xi \leqslant 10$, (2.5) was used for γ and the integral in (1.11) was performed directly. For $\xi > 10$, the independent variable was changed to $\rho = \log_{10}\xi$, and (3.23) was used for V (with $\gamma = V/\xi$). The result of the integration is shown in figure 6 for values of β' up to 1000. In order to see if (4.2) gives a good description of this curve, we proceed as in I, setting $\beta = b\beta''$ and choosing b so that the value of β' when $\gamma_l = 0{\cdot}5$ from figure 6 is the same as the value of β'' when $\gamma_l = 0{\cdot}5$ from (4.2); this gives $b = 0{\cdot}586$. It then turns out that the graph of γ_l against β'' computed from (4.2) is virtually indistinguishable from that of figure 6;

table 2 shows how close the coincidence between the two curves is for $\beta' = \beta'' \leqslant 500$. We have thus demonstrated that, in this case too, equation (4.2) *can* be used to describe the effect of the 'unstirred' concentration boundary layer, as long as the layer thickness δ, used in the definition of β (equation (4.3)), is given by

$$\delta = 0{\cdot}586 \times 9^{\frac{1}{3}}\delta_c = 1{\cdot}22(Dl/\alpha)^{\frac{1}{3}}, \tag{4.4}$$

at least as long as β' is less than about 500 ($\beta \lesssim 300$).

What value is β' likely to attain in a realistic experiment? As in I, we suppose $D = 5 \times 10^{-6}\,\mathrm{cm^2\,s^{-1}}$ (as for sucrose), $C_b = 3 \times 10^{-4}\,\mathrm{mol\,cm^{-1}}$ and maximum values for P are $6 \times 10^{-1}\,\mathrm{cm\,s^{-1}\,(mol\,cm^{-3})^{-1}}$ for a cell membrane and $4{\cdot}4\,\mathrm{cm\,s^{-1}\,(mol\,cm^{-3})^{-1}}$ for rat kidney proximal tubule (House 1974). Schafer, Patlak & Andreoli (1974) performed experiments with rabbit proximal tubule, perfusing it at a flow rate of about $30\,\mathrm{nl\,min^{-1}}$; the diameter of such a tubule is about $20\,\mu\mathrm{m}$, so α turns out to be about $5000\,\mathrm{s^{-1}}$. The lengths of the tubule segments used by Schafer *et al.* were up to 4 mm. The highest value of P quoted above leads to a value for β' of approximately 1·2. Everitt, Redwood & Haydon (1969) mounted an artificial membrane in the boundary of a cylinder containing a concentric rotating cylinder in such a way that it would experience a uniform shear flow; in their case l was 1 mm and α at least $3\,\mathrm{s^{-1}}$. Taking $P = 0{\cdot}6\,\mathrm{cm\,s^{-1}\,(mol\,cm^{-3})^{-1}}$, we obtain $\beta' \approx 0{\cdot}4$. Thus practical values of β' lie well within the range of values covered by this theory (indeed, the small-ξ theory would be sufficiently accurate in the above cases), but they are not so small that the reduction in osmotic flux below the value given by (1.1) with $\Delta C = C_b$ is insignificant.

Finally, we should check that the inequalities (1.3) and (1.4) are satisfied in the above practical examples, for if not the assumption that the flow in the concentration boundary layer can be described by the given uniform shear plus the osmotic flux will not be justified. The right-hand side of (1.4) turns out always to be very large (equal to $2{\cdot}7 \times 10^6$ for the experiments of Schafer *et al.*, and to 460 for those of Everitt *et al.*), but the right-hand side of (1.3) is rather smaller (equal to 1·8 for Schafer *et al.* and 83 for Everitt *et al.*). Thus (1.3) is not clearly satisfied for Schafer *et al.*'s experiments on kidney proximal tubule; the reason is that h, the radius of the tubule, is so small that the osmotic flux can have a significant effect on the flow rate down the tubule. Furthermore the concentration boundary-layer thickness δ_c (1.2) will have become approximately equal to h ($\approx 10\,\mu\mathrm{m}$) at the downstream end of their 4 mm segment. The present theory would, of course, be applicable for shorter lengths of tubule, for which β' was smaller than the value quoted above. A new theory for a long segment will probably be quite feasible because the Reynolds number of flow in the tubule is sufficiently small that lubrication theory can be applied.

REFERENCES

Abramowitz, M. & Stegun, I. A. 1964 *Handbook of Mathematical Functions*. Washington: National Bureau of Standards.

Domb, C. & Sykes, M. F. 1957 On the susceptibility of a ferromagnetic above the Curie point. *Proc. Roy. Soc.* **A 240**, 214–228.

Everitt, C. T., Redwood, W. R. & Haydon, D. A. 1969 Problem of boundary layers in the exchange diffusion of water across bimolecular lipid membranes. *J. Theor. Biol.* **22**, 20–32.

Gill, W. N., Tien, C. & Zeh, D. W. 1966 Analysis of continuous reverse osmosis systems for desalination. *Int. J. Heat Mass Transfer* **9**, 907–923.

HENDRICKS, T. J. & WILLIAMS, F. A. 1971 Diffusion-layer structure in reverse osmosis channel flow. *Desalination* **9**, 155–180.

HOUSE, C. R. 1974 *Water Transport in Cells and Tissues*. London: Edward Arnold.

LÉVÊQUE, M. A. 1928 Transmission de chaleur par convection. *Ann. des Mines* **13**, 201–362.

PEDLEY, T. J. 1980 The interaction between stirring and osmosis. Part 1. *J. Fluid Mech.* **101**, 843–861.

SCHAFER, J. A., PATLAK, C. S. & ANDREOLI, T. E. 1974 Osmosis in cortical collecting tubules. *J. Gen. Physiol.* **64**, 201–227.

SMITH, F. T. 1976 Flow through constricted or dilated pipes and channels. I. *Quart. J. Mech. Appl. Math.* **29**, 343–364.

VAN DYKE, M. 1975 *Perturbation Methods in Fluid Mechanics*, 2nd edn. Parabolic.